Dioxygen Insertion into Iron(III)-Carbon Bonds. NMR Studies of the Formation and Reactivity of Alkylperoxo Complexes of Iron(III) Porphyrins†

Ramesh D. Arasasingham, Alan L. Balch,* Charles R. Cornman, and Lechoslaw Latos-Grazynski

Contribution from the Department of Chemistry, University of California, Davis, California 95616. *Received June 15, 1988*

Abstract: The behavior of $PFe^{III}CHR_2$ (P is a porphyrin dianion) in solution especially in the presence of dioxygen has been examined by ^1H and ^2H NMR measurements. Evidence for the photolytic Fe–C bond homolysis with the formation of PFe^{II} is presented. Addition of dioxygen to $PFeCH_2R$ produces two unstable intermediates, $PFe^{III}O_2CH_2R$ and $PFe^{III}OH$, which may be directly observed at low temperatures. These form and decompose through the following reactions: $PFe^{III}CH_2R + O_2 \rightarrow PFe^{III}O_2CHR_2$; $PFe^{III}O_2CHR_2 \rightarrow PFe^{III}OH + O{=}CR_2$; $2PFe^{III}OH \rightarrow PFe^{III}OFe^{III}P + H_2O$. The formation of the product aldehyde or ketone has been established for methyl, ethyl, isopropyl, *n*-propyl, and benzyl ligands axially coordinating iron. The dioxygen insertion is retarded by the coordination of *N*-methylimidazole to the sixth iron coordination site or by employing a sterically encumbered porphyrin. $PFe^{III}OH$ catalyzes the decomposition of ethyl hydroperoxide to give acetaldehyde as the major organic product.

This article is concerned with the chemical behavior of two functional groups, iron alkyls and iron alkylperoxo complexes, which are of considerable current interest in bioinorganic chemistry.

Iron alkyl complexes have only recently become significant in this context. Four broad classes of iron alkyls can be identified: the large group of conventional diamagnetic, low-valent complexes with 18-electron configurations,[1] a smaller class of five-coordinate iron(III) alkyls with only 15 electrons,[2-7] an even smaller class of paramagnetic four-coordinate iron(II) alkyls with 14 electrons,[8,9] and the unique tetrakis(norbornyl)iron(IV).[10] It is the second class of five-coordinate iron(III) complexes that includes alkyl iron(III) porphyrin complexes ($PFe^{III}R$) that are of interest here. These complexes fall into two subgroups, which may be either low spin ($S = {}^1/_2$)[2-5] or high spin ($S = {}^5/_2$),[6,7] depending on the identity of the alkyl group or the tetradentate ligand that completes the iron coordination. Complexes of the $PFe^{III}R$ type have been identified as products of biologically significant reactions. Treatment of heme proteins or iron porphyrin models with substituted hydrazines (important since that functionality is present in certain drugs) or diazenes (their oxidation products) can produce the iron(III) alkyls.[11,12] Metabolism of the anesthetic halothane ($CF_3CHClBr$) has been shown to yield complexes of the type $PFe^{III}CHClCF_3$.[13-15] Anaerobic reduction of benzyl halides by microsomal cytochrome P450 is believed to involve a porphyrin iron(III) benzyl complex.[16]

Additionally, iron alkyl complexes with unspecified oxidation and ligation states have been proposed as intermediates in a variety of biologically significant reactions including penicillin biosynthesis (where the transformation Fe=O + H–C– → HO–Fe–C– has been proposed in the action of isopenicillin N synthase) and fatty acid lipoxygenation.[18] Related metallocyclic units have been proposed to form in cytochrome P450 mediated olefin epoxidation due to the 2 + 2 cycloaddition of a ferryl (FeO^{2+}) unit with an olefin.

Hydroperoxide and alkyl hydroperoxide complexes of iron are of obvious significance in the mechanism of action of heme proteins (catalase and the peroxidases).[19,20] Peroxo intermediates have also been suggested to be involved in lipoxygenation[18] and in the conversion of androgens to estrogens by the P450 enzyme estrogen synthetase (aromatase).[21,22]

The work described here involves detection of intermediates and products formed by the addition of dioxygen to low-spin $PFe^{III}R$ complexes. A preliminary report has appeared.[23] These iron(III) complexes are very reactive toward dioxygen. Their behavior should be compared to that of the related and much more intensively studied cobalt alkyl complexes (vitamin B_{12} models) which undergo dioxygen insertion only after photolysis homolytically ruptures the Co–C bond.[24] Thus, with cobalt, chiral alkyl groups are racemized during the dioxygen insertion.[25]

† Abbreviations used: P, a porphyrin dianion; TTP, dianion of tetra-*p*-tolylporphyrin; TMP, dianion of tetramesitylporphyrin; R, alkyl group or hydrogen.

(1) Johnson, M. D. *Comprehensive Organometallic Chemistry*; Wilkinson, G., Stone, F. G. A., Abel, E. W., Eds.; Pergamon Press: New York, 1982; Vol. 4, p 331.
(2) Clark, D. A.; Dolphin, D.; Grigg, R.; Johnson, A. W.; Pinnock, H. A. *J. Chem. Soc. C* **1968**, 881.
(3) Lexa, D.; Mispelter, J.; Saveant, J.-M. *J. Am. Chem. Soc.* **1981**, *103*, 6806. These authors did not observe the β-protons of the axial ethyl or *n*-butyl groups in $PFe^{III}R$.
(4) Cocolios, P.; Laviron, E.; Guilard, R. *J. Organomet. Chem.* **1982**, *228*, C39.
(5) Cocolios, P.; Lagrange, G.; Guilard, R. *J. Organomet. Chem.* **1983**, *253*, 65.
(6) Floriani, C.; Calderazzo, F. *J. Chem. Soc. A* **1971**, 3665.
(7) Tabard, A.; Cocolios, P.; Lagrange, G.; Gerardin, R.; Hubsch, J.; Lecomte, C.; Zarembowitch, J.; Guilard, R. *Inorg. Chem.* **1988**, *27*, 110.
(8) Hermes, A. R.; Girolami, G. S. *Organometallics* **1987**, *6*, 763.
(9) Hill, D. H.; Sen, A. *J. Am. Chem. Soc.* **1988**, *110*, 1650.
(10) Bowser, B. K.; Tennent, H. G. *J. Am. Chem. Soc.* **1972**, *94*, 2512.
(11) Battioni, P.; Mahy, J.-P.; Gillet, G.; Mansuy, D. *J. Am. Chem. Soc.* **1983**, *105*, 1399.
(12) Battioni, P.; Mahy, J.-P.; Delaforge, M.; Mansuy, D. *Eur. J. Biochem.* **1983**, *134*, 241.
(13) Ahr, H. J.; King, L. J.; Nastainczyk, W.; Ullrich, V. *Biochem. Pharmacol.* **1980**, *29*, 2855.
(14) Rub, H. H.; Ahr, H.; Nastainczyk, W.; Ullrich, V.; Mansuy, D.; Battioni, J.-P.; Montiel-Montoya, R.; Trautwein, A. *Biochemistry* **1984**, *23*, 5300.
(15) Mansuy, D.; Battioni, J.-P. *J. Chem. Soc., Chem. Commun.* **1982**, 638.
(16) Mansuy, D.; Fontecave, M. *Biochem. Pharmacol.* **1983**, *32*, 1871.
(17) Baldwin, J. E. *Recent Advances in the Chemistry of β-Lactam Antibiotics*; Brown, A. G., Roberts, S. M., Eds.; Royal Society of Chemistry: London, 1985; p 62.
(18) (a) Corey, E. J.; Nagata, R. *J. Am. Chem. Soc.* **1987**, *109*, 8107. (b) Corey, E. J.; Walker, J. C. *J. Am. Chem. Soc.* **1987**, *109*, 8108.
(19) Hewson, W. D.; Hager, L. P. In *The Porphyrins*; Dolphin, D., Ed.; Academic Press: New York, 1979; Vol. 7, p 295.
(20) Marnett, L. J.; Weller, P.; Battista, J. R. In *Cytochrome P450: Structure, Mechanism and Biochemistry*; Ortiz de Montellano, Ed.; Plenum Press: New York, 1986; p 29.
(21) Akhtar, M.; Calder, M. R.; Cortin, D. L.; Wright, J. N. *J. Chem. Soc., Chem. Commun.* **1981**, 129. Stevenson, D. E.; Wright, J. N.; Akhtar, M. *J. Chem. Soc., Chem. Commun.* **1985**, 1078.
(22) Cole, P. A.; Robinson, C. H. *J. Am. Chem. Soc.* **1988**, *110*, 1284.
(23) Arasasingham, R. D.; Balch, A. L.; Latos-Grazynski, L. *J. Am. Chem. Soc.* **1987**, *109*, 5846.
(24) Toscano, P. J.; Marzilli, L. G. *Prog. Inorg. Chem.* **1984**, *31*, 105.
(25) Denaiu, J.; Gaudemer, A. *J. Organomet. Chem.* **1980**, *191*, C1.

0002-7863/89/1511-4357$01.50/0

Table I. ^{1}H NMR Data for PFe^{III}R and PFe^{III}OR Complexes

compd	temp, °C	chem shift,[a] ppm				
		R/OR	pyrrole	phenyl substituents		
				ortho	meta	para[b]
(TTP)FeCH$_3$	−70		−34	−1.8, 0.3	1.8, 2.2	−1.0
(TMP)FeCH$_3$	−70		−35	−1.1, −0.4	1.4, 1.5	−0.8
(TTP)FeC$_2$H$_5$	−70	β, −154	−34	−1.9, 0.1	1.7, 2.1	−1.1
(TTP)FeC$_3$H$_7$ (*n*)	−70	β, −27 γ, 12	−35	−2.1, 0.1	1.6, 2.1	−1.2
(TTP)FeCH(CH$_3$)$_2$	−70	β, −154	−34	−1.9, 0.1	1.7, 2.1	−1.1
(TTP)FeCH$_2$C$_6$H$_5$	−70	*o*, 72 *m*, 3.6 *p*, 52	−33	−1.1	2.4	−0.9
(*N*-MeIm)(TTP)FeCH$_3$	−70		−37	−2.5, −2.9	1.5, 1.6	−1.4
(*N*-MeIm)(TTP)FeC$_2$H$_5$	−70	β, −94	−36	−2.6, −2.2	1.5, 1.6	−1.3
(TMP)FeOCH$_3$	24		80	*c*	11.7, 10.9	3.3
(TTP)FeOC$_2$H$_5$	24	β, 22	80	*c*	10.5, 9.7	4.5
(TMP)FeOC(CH$_3$)$_3$	24	β, 34	80	*c*	12.1, 10.9	3.3
	−70	β, 47	116	*c*	20.3, 17.7	5.1
(TMP)FeOH	−60		111	*c*	14.3, 13.0	3.9
(TMP)FeOC$_2$H$_5$	−60	β, 32	111	*c*	14.3, 13.0	3.9

[a] In toluene-d_8. [b] Methyl resonance. [c] Not observed.

Results

NMR Spectra for Isolated Iron(III) Alkyl and Alkoxy Complexes. Table I contains the NMR spectral data for (TTP)Fe^{III}R (**1**-R) and (TTP)Fe^{III}OR, which were obtained by standard methods.[3-5,26] The alkyl complexes have ^{1}H NMR resonance patterns (see trace A of Figure 1) that are consistent with a low-spin ($S = {}^1/_2$) structure with a pyrrole resonance at ca. −19 ppm. Our observations are consistent with previous reports on the methyl, ethyl, and *n*-butyl complexes ((TTP)Fe^{III}R).[3-5,26] The propyl, isopropyl, and benzyl complexes have not previously been reported but the resonance patterns are consistent with their structures. In no case have resonances for α-CH$_3$ or α-CH$_2$ groups been observed. Additional attempts to detect these by ^{2}H NMR, which can facilitate the detection of paramagnetically broadened resonances, were also unsuccessful. Careful examination of the ^{2}H NMR spectra of **1**-CD$_3$ or **1**-CD$_2$CD$_3$ in the region +250 to −250 ppm revealed only the resonance of the β-CD$_3$ group of **1**; no resonance of the α-CD$_3$ or α-CD$_2$ groups could be seen. In our hands, it has not been possible to prepare iron(III) complexes with the axial alkyl group lacking α-protons presumably for steric reasons. Extensive attempts to prepare (TTP)Fe^{III}C(CH$_3$)$_3$ from the reaction of (TTP)Fe^{III}Cl and the Grignard reagent derived from *tert*-butyl bromide did not yield a solution with ^{1}H NMR resonances consistent with the presence of the desired iron(III)–*tert*-butyl complex. The major product was (TTP)Fe^{II}, which may have arisen from decomposition of the iron(III)–*tert*-butyl complex. Similarly, attempts to obtain (TTP)Fe^{III}CF$_3$ from the reaction of (TTP)Fe^{I}[4,27] with trifluoromethyl iodide did not yield the desired product.

In contrast to these alkyl complexes, the alkoxy complexes are high-spin ($S = {}^5/_2$) species.[26,28] As such, they display a broad pyrrole resonance at ca. 80 ppm at 24 °C. Axial ligand resonances for the β-CH$_3$ groups of the ethoxy and *tert*-butoxy complexes appear at 21 and 34 ppm, respectively. Resonances of the α-CH$_2$ group of the ethoxy and the α-CH$_3$ of the methoxy complex have not been detected even by ^{2}H NMR spectroscopy of (TTP)Fe^{III}OCD$_2$CD$_3$.

Solution Behavior of Porphyrin Iron(III) Alkyl Complexes. Trace A of Figure 1 shows the 360-MHz ^{1}H NMR spectrum of (TTP)Fe^{III}C$_2$H$_5$ (**1**-C$_2$H$_5$) at 23 °C in toluene-d_8 solution. This solution of **1**-C$_2$H$_5$ contains traces of (TTP)Fe^{II} (**2**), which arises from the decomposition of **1**-C$_2$H$_5$, and of (TTP)Fe^{III}OFe^{III}TTP (**5**), which comes from reaction of **1** or **2** with small amounts of adventitious dioxygen. The NMR spectra of both **2**[29] and **5**[30] have been obtained and analyzed previously. In the absence of light and dioxygen this solution of the alkyl complex shows no decay over a several-day period. However, exposure to light does alter the solution. Trace B shows the spectrum of the solution of **1**-C$_2$H$_5$ after exposure to light for 18 h. The intensities of all resonances due to **1** have decreased while the resonances due to the iron(II) complex, **2**, have increased significantly. Since our septum-capped NMR tubes are not completely impervious to dioxygen, some increase in the concentration of the μ-oxo dimer **5** also occurs. Further irradiation produces more **2**. When the NMR spectrum

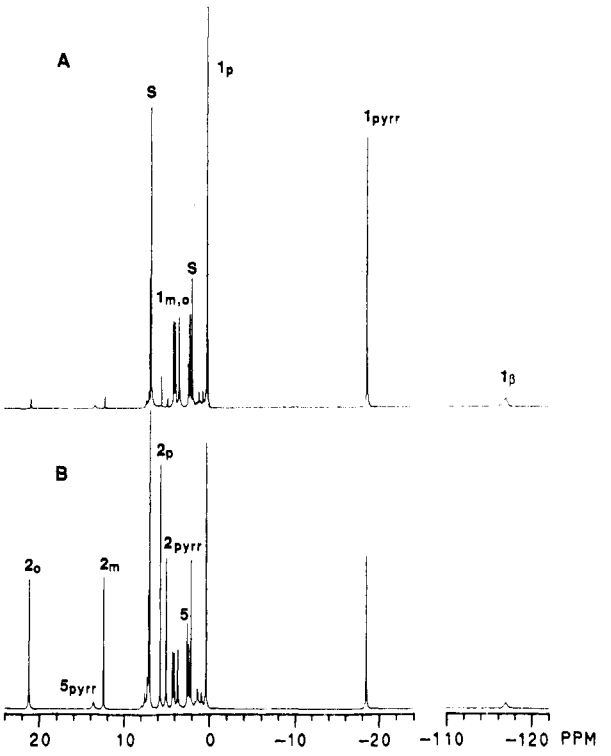

Figure 1. 360-MHz ^{1}H NMR spectra of (TTP)Fe^{III}CH$_2$CH$_3$ (**1**-C$_2$H$_5$) in toluene-d_8 at 23 °C: (A) fresh sample after chromatography; (B) the same sample after exposure to unfiltered light for 18 h. Peaks due to (TTP)Fe^{III}CH$_2$CH$_3$ are labeled 1, those of (TTP)Fe^{II}, 2; and those of (TTP)Fe^{III}OFe^{III}(TTP), 5. Subscripts refer to assignments : β, ethyl CH$_3$; pyrr, pyrrole; o, ortho phenyl; m, meta phenyl; p, para methyl protons.

(26) Arafa, I. M.; Goff, H. M.; David, S. S.; March, B. P.; Que, L., Jr. *Inorg. Chem.* **1987**, *26*, 2779.
(27) Mashiko, T.; Reed, C. A.; Haller, K. J.; Scheidt, W. R. *Inorg. Chem.* **1984**, *23*, 3192.
(28) Kobayashi, H.; Higuchi, T.; Kaizu, Y.; Osuda, H.; Aoki, M. *Bull. Chem. Soc. Jpn.* **1975**, *48*, 3137.
(29) Goff, H.; La Mar, G. N.; Reed, C. A. *J. Am. Chem. Soc.* **1977**, *99*, 3641.
(30) La Mar, G. N.; Eaton, G. R.; Holm, R. H.; Walker, F. A. *J. Am. Chem. Soc.* **1973**, *95*, 63.

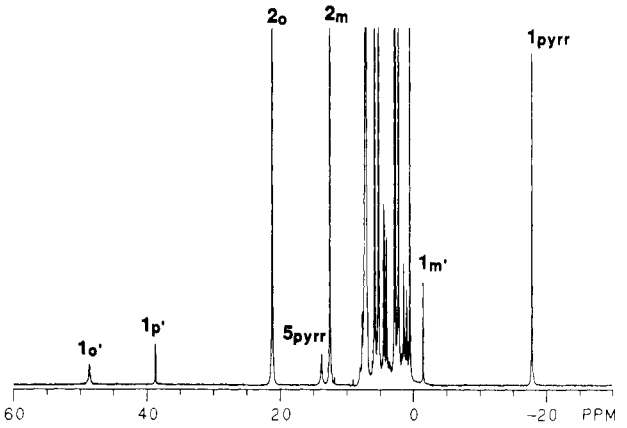

Figure 2. 360-MHz ^{1}H NMR spectrum of a sample of (TTP)Fe^{III}C-$H_2C_6H_5$ in toluene-d_8 at 23 °C. Peaks due to (TTP)Fe$^{III}CH_2C_6H_5$ are labeled 1; those of (TTP)Fe^{II} are labeled 2. Subscripts refer to assignments, as in Figure 1 with the following additions: o', ortho benzyl phenyl protons; m', meta benzyl phenyl protons; p', para benzyl phenyl protons.

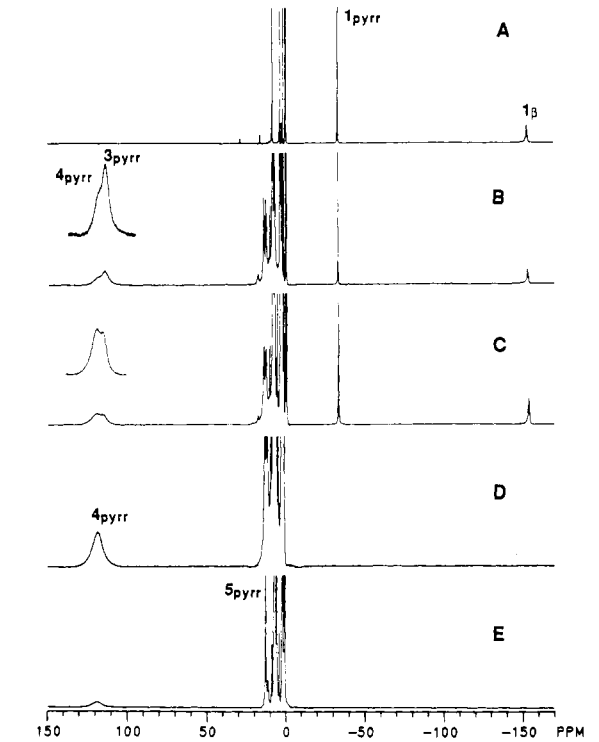

Figure 3. 360-MHz ^{1}H NMR spectra obtained from the reaction between (TTP)Fe$^{III}CH_2CH_3$ and O_2 at −70 °C in toluene-d_8 solution: (A) (TTP)Fe$^{III}CH_2CH_3$ alone; (B,C) successive spectra run after the addition of dioxygen over a 2-h period with the sample in a −80 °C bath and recorded at −70 °C; (D) the sample after warming to −60 °C and cooling to −70 °C; (E) the sample after warming to room temperature and immediately cooling to −70 °C. Peaks of (TTP)Fe$^{III}CH_2CH_3$ are labeled 1; those of (TTP)Fe$^{III}OOCH_2CH_3$, 3; those of (TTP)Fe^{III}OH, 4; and those of (TTP)Fe^{III}OFe^{III}(TTP), 5. Subscripts are used as given in Figure 1.

is collected under diamagnetic conditions, ethane (but not ethylene) can be detected. These results indicate that light induces homolytic cleavage of the Fe–C bond according to eq 1.

$$\underset{\mathbf{1}}{(\text{TTP})\text{Fe}^{III}\text{CH}_2\text{CH}_3} \xrightarrow{h\nu} \underset{\mathbf{2}}{(\text{TTP})\text{Fe}^{II}} + {}^{\bullet}\text{CH}_2\text{CH}_3 \qquad (1)$$

Similar behavior has been observed for iron(III) complexes with methyl, propyl, or isopropyl axial ligands. In each case in the absence of light and dioxygen, the iron(III) alkyl is stable in solution for at least periods of days.

We have prepared samples of the benzyl complex (TTP)-Fe$^{III}CH_2C_6H_5$ from (TTP)Fe^{III}Cl and $BrMgCH_2Ph$. In solution this is much less stable than the methyl, ethyl, or propyl complexes described above. Even when protected from light, samples of **1**-$CH_2C_6H_5$ are invariably accompanied by large amounts of (TTP)Fe^{II}. In fact, in most cases (TTP)Fe^{II} is the major constituent of the sample as is seen in Figure 2, which shows the ^{1}H NMR spectrum obtained from a typical sample of **1**-$CH_2C_6H_5$. Nevertheless, characteristic resonances of **1**-$CH_2C_6H_5$ have been detected and assigned. The resonances of the phenyl protons of the benzyl group are easily resolved. The para resonance is readily assigned on the basis of intensity, and the ortho resonance is differentiated from the meta resonance on the basis of the larger line width. Since the ortho and para protons have opposite shifts from the meta protons, it appears that there is π-spin delocalization into this phenyl ring. As expected, the α-CH_2 resonances are not observed. Decomposition of **1**-$CH_2C_6H_5$ yields bibenzyl (as determined by ^{1}H NMR) along with (TTP)Fe^{II}.

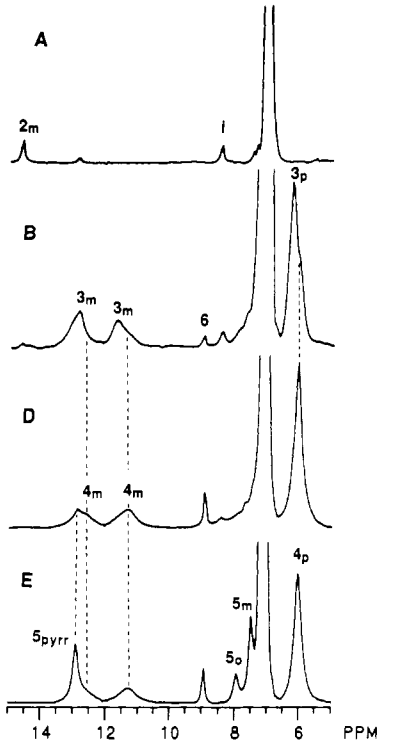

Figure 4. The 5–15 ppm region of the 360-MHz ^{1}H NMR spectrum obtained from the reaction between (TTP)Fe$^{III}CH_2CH_3$ and O_2 at −70 °C in toluene solution. Traces A, B, D, and E are expansions of traces A, B, D, and E in Figure 3. Thus trace A shows the spectrum of (TTP)Fe$^{III}CH_2CH_3$, traces B and D are run in the presence of O_2, and trace E is obtained after warming to 25 °C and recooling to −70 °C. Labeling follows from that in Figures 1 and 2 with the peak labeled 6 resulting from acetaldehyde.

Reaction of (TTP)Fe^{III}R with Dioxygen. Addition of dioxygen to a toluene-d_8 solution of (TTP)Fe$^{III}CH_2CH_3$ produces the spectral changes shown in Figures 3 and 4. Figure 3 shows the entire spectrum, while Figure 4 presents an expansion of the 5–15 ppm region. Trace A in both figures shows the spectrum of (TPP)Fe$^{III}C_5H_5$ at −70 °C before the addition of dioxygen. Trace B shows the spectrum immediately after the addition of dioxygen to the sample. In Figure 3, two new pyrrole resonances at ca. 120 ppm have grown into the spectrum. These are assigned to two intermediates, (TTP)Fe$^{III}OOCH_2CH_3$ (**3**-CH_2CH_3) and (TTP)Fe^{III}OH (**4**).[31,32] The line widths of these resonances, ca. 1600 Hz, are consistent with axial ligation of oxygen donors. Trace C of Figure 3 shows a further stage in the reaction in which the intensity of the two pyrrole resonances are more nearly equal. (TTP)FeOOC_2H_5 is stable at −70 °C for several hours. Trace D shows the sample after warming to −60 °C and recooling

(31) Cheng, R.-J.; Latos-Grazynski, L.; Balch, A. L. *Inorg. Chem.* **1982**, *21*, 2412.
(32) Fielding, L.; Eaton, G. R.; Eaton, S. S. *Inorg. Chem.* **1985**, *24*, 2309.

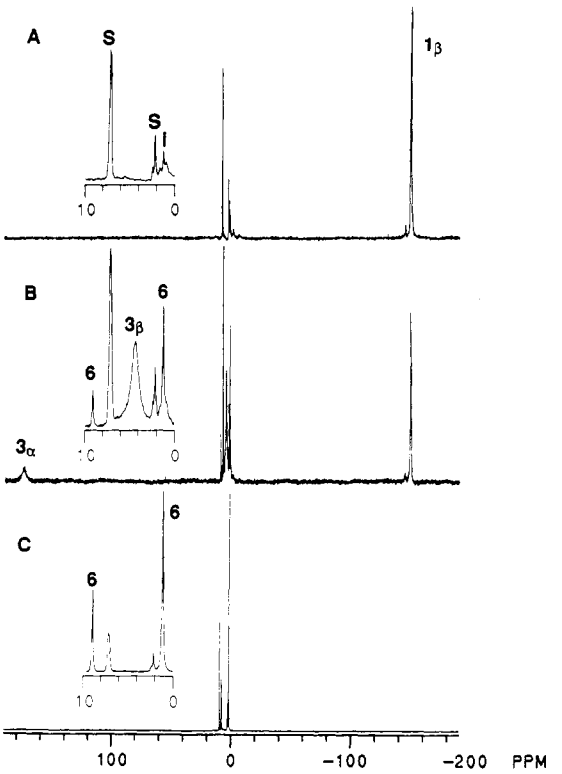

Figure 5. 76-MHz ^2H NMR spectra obtained from the reaction of (TTP)$Fe^{III}CD_2CD_3$ and O_2 at −70 °C in toluene solution: (A) (TTP)$Fe^{III}CD_2CD_3$ alone; (B) the sample after the addition of O_2; (C) the same sample after 2 h. Insets show expansions of the 0–10 ppm region. Peaks of (TTP)$FeCD_2CD_3$ are labeled 1; those of (TTP)$Fe^{III}OOCD_2CD_3$, 3; and those of acetaldehyde, 6. Subscripts α and β refer to methylene and methyl protons, respectively.

immediately. All of the original sample of the ethyl complex **1** has reacted and the intermediate **3**-CH_2CH_3 also has disappeared. Trace E shows the spectrum of the sample after warming to 25 °C and recooling to −70 °C. The intensity of the pyrrole resonance of **4** has decreased, while the intensity of a pyrrole resonance at 13 ppm, due to (TTP)$Fe^{III}OFe^{III}$TTP (**5**), has grown considerably (see Figure 4 as well).

Figure 4 clarifies a portion of these spectra. Comparing the spectra in trace A (taken before dioxygen addition) and trace B (taken after dioxygen addition), one can see the growth of resonances in the 11–13 ppm region where *m*-phenyl resonances of high-spin, five-coordinated iron(III) porphyrins are expected. The asymmetry of these is due to overlapping of the peaks of the two intermediates, **3**-CH_2CH_3 and **4**. Similarly, in the 6–7 ppm region one sees two new resonances due to the methyl groups of the *p*-tolyl substituents. Notice also that a new resonance, **6**, has grown into the spectrum. This is due to the aldehyde proton of acetaldehyde, which is formed from the ethyl group. This resonance appears artificially broadened in these spectra because they were acquired under conditions suitable for detecting the broad paramagnetic resonances. On standing for 2 h at −70 °C the spectrum undergoes the conversion from trace B to trace D. The intensity of the resonances due to (TTP)Fe^{III}OH (**4**) and acetaldehyde (**6**) grow, while those of (TTP)$Fe^{III}OOCH_2CH_3$ (**3**-CH_2CH_3) disappear. Warming to 25 °C and then recooling to −70 °C produces the changes seen on going from trace D to trace E. The intensities of the resonances of **4** decrease, while resonances of **5**, the ubiquitous μ-oxo dimer, increase.

In order to directly observe the changes in the axial ethyl group throughout this process, the ^2H NMR spectrum of (TTP)$Fe^{III}CD_2CD_3$ has been recorded under similar conditions. The ^2H NMR spectrum of **1**-CD_2CD_3 in toluene at −70 °C is shown in trace A of Figure 5. In addition to resonances at 7 and 1–2 ppm due to solvent and solvent impurities, a singlet at −145 ppm is observed for β-CD_3 protons. The much smaller peak at −140 ppm is assigned to the β-CD_2H resonance of a small quantity of

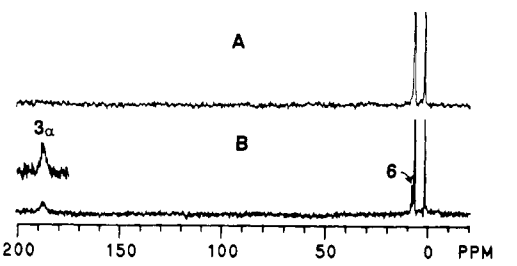

Figure 6. ^2H NMR spectra obtained from the reaction of (TTP)$Fe^{III}CD_3$ and O_2 at −70 °C in toluene solution: (A) (TTP)$Fe^{III}CD_3$ alone; (B) the sample after the addition of O_2. Labeling follows that in Figure 5 except 6 refers to formaldehyde.

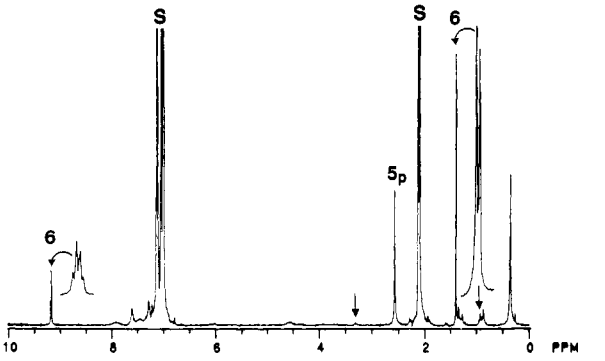

Figure 7. ^1H NMR spectrum obtained from a sample of (TTP)$Fe^{III}C-H_2CH_3$ in toluene-d_8 at 25 °C after treatment with dioxygen. Resonance labels follow those in previous figures.

(TTP)$Fe^{III}CD_2CD_2H$ that arises from incomplete deuteration of the ethyl iodide used in the preparation of **1**-CD_2CD_3. The large isotope effect seen here is entirely consistent with other observations of ^1H isotope effects on ^2H NMR spectra of paramagnetic compounds.[33] On addition of dioxygen at −70 °C, the spectrum is transformed into that seen in trace B. New broad resonances at 180 and 4 ppm have developed in the spectrum. These are assigned to the CD_2 and CD_3 resonances, respectively, of the alkylperoxo ligand in (TTP)$Fe^{III}OOCD_2CD_3$. Additionally, narrow resonances at 9.5 and 1.5 ppm have appeared in trace B. These are due to the aldehyde and methyl resonances of acetaldehyde. After this sample was warmed to 25 °C and recooled to −70 °C, its spectrum was transformed into that seen in trace C of Figure 5. At this stage the broad resonances of both **1** and **3**-CD_2CD_3 are gone. Only the narrow resonances of acetaldehyde remain. Notice in the inset that the intensities of these acetaldehyde resonances greatly exceed those of the solvent and solvent impurities in trace C.

In order to confirm the resonance assignments for the ethylperoxo ligand in (TTP)$Fe^{III}OOCD_2CD_3$, we examined the effect of oxygenation of (TTP)$Fe^{III}CD_3$. Trace A of Figure 6 shows the ^2H NMR spectrum of **1**-CD_3 in toluene at −70 °C. Only resonances due to solvent and solvent impurities are seen. Trace B shows the spectrum obtained after the addition of dioxygen. A broad new resonance appears at 188 ppm. This is assigned to the $OOCD_3$ resonance of **3**-CD_3. A narrow resonance at 9 ppm due to formaldehyde-d_2 also appears. On further standing, the broad resonance at 188 ppm eventually disappears, and the resonance at 9 ppm grows in intensity. It should be noted that the resonances seen in Figures 5 and 6 for the $OOCD_2CD_3$ and $OOCD_3$ groups are quite distinct from the resonances expected for the OCD_2CD_3 and OCD_3 groups in the alkoxy complexes (TTP)Fe^{III}OR (see Table I).

Careful examination of the 0–10 ppm region of the ^1H NMR spectra of the reaction products (taken under diamagnetic conditions at 25 °C after oxygenation was complete) allows the identification of the organic products arising from the axial alkyl group. Figure 7 shows data obtained from the dioxygen/

(33) Horn, R. R.; Everett, G. W., Jr. *J. Am. Chem. Soc.* **1971**, *93*, 7173.

$(TTP)Fe^{III}CH_2CH_3$ reaction. Resonances due to acetaldehyde are labeled 6. The spin–spin coupling observed in the insets, along with the chemical shifts, readily identifies the product. Our ability to detect well-resolved resonances for these diamagnetic products in the presenct of the antiferromagnetic $(TTP)Fe^{III}OFe^{III}(TTP)$ is due to two factors. Simple aldehydes (or ketones) are poor ligands. Moreover, the μ-oxo dimer $(TTP)Fe^{III}OFe^{III}P$ shows little ability to coordinate an additional axial ligand. Small amounts of ethanol are also observed in this sample. These resonances are identified by the downward-pointing arrows in Figure 7. The ratio of acetaldehyde to ethanol is 96/4. No other organic product can be detected. The temperature at which the oxygenation is performed has no effect on these products or their distribution. The same results are obtained when dioxygen is introduced to a sample of **1**-CH_2CH_3 at −80 °C and then warmed as when dioxygen is admitted to a sample of **1**-CH_2CH_3 at 25 °C.

Similar results have been obtained for other alkyl groups. ^1H NMR data relating to the peroxo intermediates are given in Table I. The reaction of **1**-CH_3 yields formaldehyde (singlet at 8.6 ppm). The oxygenation of **1**-*n*-C_3H_7 yields propionaldehyde (9.2 ppm, t, 1.1 Hz; 1.7 ppm, q of d; 0.7 ppm, t, 7.3 Hz), while with **1**-*i*-C_3H_7, acetone (1.6 ppm, singlet) is formed. In the case of **1**-CH_2Ph both benzaldehyde (9.6 ppm) and bibenzyl (2.72 ppm) are observed in the ^1H NMR spectrum of the product mixture. Bibenzyl is unavoidably formed from the thermal decomposition of **1**-CH_2Ph, but the benzaldehyde is formed only when the sample is exposed to dioxygen.

With the sterically hindered porphyrin complex (TMP)-$Fe^{III}CH_3$, the dioxygen reaction requires higher temperatures to achieve reactions comparable to those seen with $(TTP)Fe^{III}CH_3$. Addition of dioxygen to a toluene-d_8 solution of $(TMP)Fe^{III}CH_3$ at −50 °C produces a high-spin alkylperoxo intermediate. After standing at −50 °C for 1 h, this intermediate is converted entirely into the stable $(TMP)Fe^{III}OH$, which is unable to undergo dehydration to form a μ-oxo complex for steric reasons.[31] During this process, no other intermediates were detected. Formaldehyde was the final organic product.

Effect of Axial Base. The coordination of an additional axial ligand and the effect of that ligand on the oxygenation have been examined. Trace A of Figure 8 shows the ^1H NMR spectrum obtained from a toluene solution of $(TTP)Fe^{III}CH_2CH_3$ in the presence of 1-methylimidazole at −70 °C. The spectral pattern is similar to that observed for six-coordinate $(TMP)Fe^{III}Ph$(1-MeIm) described previously.[34] The pyrrole resonance at −36 ppm is consistent with a low-spin ($S = {}^1/_2$) structure for the six-coordinate adduct **7** via eq 2. While the addition of the axial

$$(TTP)Fe^{III}CH_2CH_3 + \text{1-MeIm} \rightleftharpoons (TTP)Fe^{III}(CH_2CH_3)(\text{1-MeIm}) \quad (2)$$

imidazole has produced an upfield shift of the pyrrole resonance from −34 to −36 ppm (compare trace A of Figure 3 to trace A of Figure 8), it has produced an even more dramatic downfield shift in the CH_3 resonance of the axial ethyl group from −154 to −94 ppm. This resonance assignment has been confirmed by observations on the corresponding $(TTP)Fe^{III}CD_3$/1-methylimidazole system. A similar spectrum is obtained, but no resonance is observed upfield of the pyrrole resonance. In trace A of Figure 8 the resonances in the 20–70 ppm region are due to coordinated 1-methylimidazole. On the basis of intensity, the resonance at 27 ppm is assigned to the methyl group of that ligand. The other three single-proton resonances have been assgined to the imidazole protons by comparsion with the detailed data available for the analogous phenyl complexes.[34] On warming above −60 °C, the resonances of the coordinated imidazole broaden due to the onset of dynamic exchange as observed for the phenyl complex. Trace B of Figure 8 shows the spectrum recorded at −30 °C where exchange has significantly broadened the resonances of **7**.

Addition of dioxygen to a sample of the six-coordinate complex **7** at −70 °C produces no change in the ^1H NMR spectrum. Thus

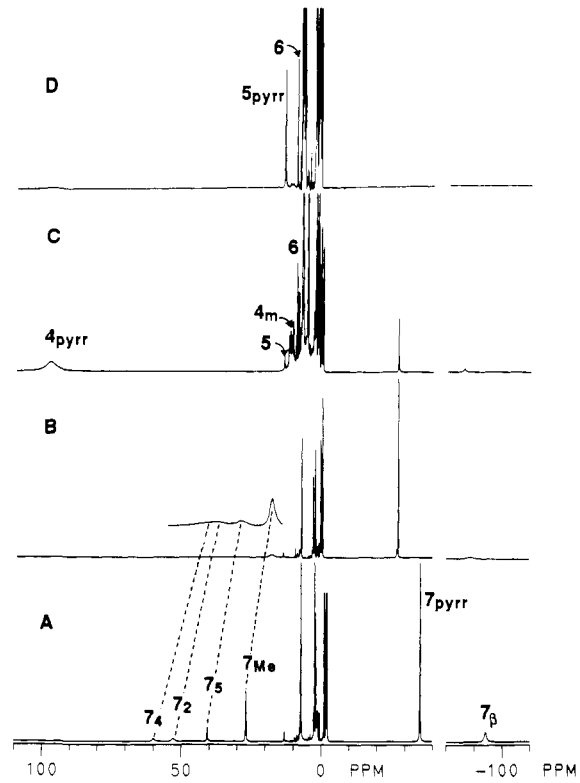

Figure 8. ^1H NMR spectra obtained from a sample of $(TTP)Fe^{III}C-H_2CH_3$ in the presence of 1 equiv of *N*-methylimidazole in toluene-d_8 solution: (A) sample at −60 °C; (B) sample at −30 °C; (C) sample at −30 °C after the addition of dioxygen; (D) sample from trace C after warming to 25 °C and recooling to −30 °C. Resonances are labeled in accord with previous figures with those of $(TTP)Fe^{III}CH_2CH_3$ (1-MeIm) labeled 7 and subscripts 2, 4, 5, and Me referring to the resonances of the imidazole protons as labeled in **7** in the text.

the six-coordinate adduct is more resistant to oxygenation than is the five-coordinate form. Upon warming, however, reaction does occur. Trace C of Figure 8 shows the spectrum obtained after the addition of dioxygen at −30 °C. New resonances appear at 97, 11.5, and 10.4 ppm that can be assigned to a high-spin ($S = {}^5/_2$), five-coordinate species. Careful examination of the line shape of these resonances indicates that only a single high-spin intermediate is present. On the basis of its further reaction (vide infra) and the previously established instability of $(TTP)Fe^{III}O-OCH_2CH_2$, this intermediate is identified as $(TTP)Fe^{III}OH$.[31,32] Additional new resonances appear at 13.3 and 9 ppm. Based on the chemical shift and its temperature dependence, the resonance at 13.3 ppm corresponds to the pyrrole resonance of (TTP)-$Fe^{III}OFe^{III}(TTP)$.[30] The resonance at 9 ppm is a quartet when recorded under diamagnetic conditions and results from the aldehyde proton of acetaldehyde. On warming, the high-spin intermediate (as well as all $(TTP)Fe^{III}CH_2CH_3$) is converted into $(TTP)Fe^{III}OFe^{III}(TTP)$ as shown in trace D of Figure 8, which shows the spectrum obtained after warming the sample to 25 °C and then recooling it to −30 °C. The major species present at this stage are $(TTP)Fe^{III}OFe^{III}(TTP)$ and acetaldehyde.

In a separate set of experiments we have reversed the sequence of additions so that at −70 °C dioxygen was reacted with (TT-P)$Fe^{III}CH_2CH_3$ to form a mixture of $(TTP)Fe^{III}OH$ and (TT-P)$Fe^{III}OOCH_2CH_3$ and then *N*-MeIm added. Under these conditions we carefully looked for the known resonances of the ferryl complex, $(TTP)Fe^{IV}{=}O$(1-MeIm),[35,36] but failed to find any of these. Rather the entire spectrum was broadened due to the independently observed equilibrium[37] shown in eq 3. Pre-

(34) Balch, A. L.; Renner, M. W. *Inorg. Chem.* **1986**, *25*, 303.

(35) Chin, D. H.; Balch, A. L.; La Mar, G. N. *J. Am. Chem. Soc.* **1980**, *102*, 1446.

(36) La Mar, G. N.; de Ropp, J. S.; Latos-Grazynski, L.; Balch, A. L.; Johnson, R. B.; Smith, K. M.; Parish, D. W.; Cheng, R. J. *J. Am. Chem. Soc.* **1983**, *105*, 782.

sumably the alkylperoxo complex was destroyed; acetaldehyde was clearly formed in the process.

$$(TTP)Fe^{III}OH + 1\text{-MeIm} \rightleftharpoons (TTP)Fe^{III}OH(1\text{-MeIm}) \quad (3)$$

Catalytic Decomposition of Ethyl Hydroperoxide. (TMP)$Fe^{III}OH$ is a catalyst for the decomposition of ethyl hydroperoxide. Acetaldehyde is the major product and no reducing agent is required to effect the decomposition. Thus treatment of a 0.06 M solution of ethyl hydroperoxide in toluene-d_8 with (TMP)$Fe^{III}OH$ (10^{-4} M) at 23 °C gave immediate evidence by ^1H NMR of the formation of acetaldehyde, and after 12 h the sample consisted of 72% acetaldehyde, 11% ethanol, and 17% ethyl hydroperoxide.

This reaction has also been monitored by ^1H NMR spectroscopy in toluene-d_8 at −60 °C as shown in Figure 9. Trace A shows the spectrum of (TMP)$Fe^{III}OH$ (**4′**) alone. Trace B shows the spectrum obtained 10 min after the addition of a tenfold excess of ethyl hydroperoxide. A new pyrrole resonance, upfield of that of **4′**, is clearly present, and a resonance at ~9 ppm due to acetaldehyde **6** has developed. On standing, as seen in trace C (30 min later) and trace D (70 min later), the upfield pyrrole resonance decays in intensity while that of (TMP)$Fe^{III}OH$ increases. However, upon addition of a second portion of ethyl hydroperoxide to the same sample, the upfield pyrrole resonance again is present. We assign this resonance to the intermediate (TMP)$Fe^{III}OOCH_2CH_3$ (**3′**). The relative positions of the pyrrole resonances in **3′** and **4′** are the same as those seen in Figure 3 for **3** and **4**; that is, the pyrrole resonances for the peroxy compounds are upfield of those of the hydroxy compounds. Thus two separate routes give rise to the alkylperoxy intermediate. It is important to notice that (TMP)$Fe^{III}OCH_2CH_3$ gives a distinct spectrum with a broad resonance at 32 ppm due to the $OCH_2\mathit{CH}_3$ protons. This resonance is absent in the spectra from which Figure 9 was derived; hence the intermediate present is not the alkoxide complex, (TMP)$Fe^{III}OCH_2CH_3$.

Discussion

The observations on the solution behavior of the iron(III) alkyl complexes reveal that for simple alkyl groups (methyl, ethyl, *n*-propyl, isopropyl) the complexes are thermally stable in toluene solution at 25 °C, but they do undergo photolytic homolysis according to eq 1 with the formation of the reactive iron(II) porphyrin clearly evident as seen in Figure 1. As a consequence, we routinely handled these iron(III) alkyl complexes in subdued light. For the benzyl complex, thermal homolytic cleavage is much more pronounced, and significant quantities of iron(II) and bibenzyl were present in all solutions of **1**-CH_2Ph that we prepared. In this case the ready cleavage of the Fe–C bond can be attributed to both the bulk of the benzyl substituent and the stability of the product—the benzyl radical.

The reaction of dioxygen with the alkyl complexes **1** is interpreted as involving three steps as shown in eq 4–6. Two unstable

$$\underset{\mathbf{1}}{PFe^{III}CHR_2} + O_2 \rightarrow \underset{\mathbf{3}}{PFe^{III}OOCHR_2} \quad (4)$$

$$\underset{\mathbf{3}}{PFe^{III}OOCHR_2} \rightarrow \underset{\mathbf{4}}{PFe^{III}OH} + O{=}CR_2 \quad (5)$$

$$2\underset{\mathbf{4}}{PFe^{III}OH} \rightarrow \underset{\mathbf{5}}{PFe^{III}OFe^{III}R} + H_2O \quad (6)$$

intermediates, **3** and **4**, are directly observed to form and then decay during the reaction. The ^1H NMR spectra for both are indicative of high-spin ($S = {}^5/_2$) species bearing an oxygen donor as the axial ligand. The hydroxy complex, **4**, has been independently prepared by the reaction between hydroxide and $PFe^{III}Cl$ at low temperature, and the conversion of this hydroxy complex into the μ-oxo dimer, **5**, via eq 6 is well established.[31,32] The alkylperoxo complex, **3**, is very unstable and can only be detected at temperatures below −70 °C. Particular care has been taken to identify the resonances of the alkylperoxo ligand. These have been identified for both the ethyl and methyl complexes and differentiate **3** from **4** and from the alkoxy complexes $PFe^{III}OR$. Reaction 4 offers a unique means for preparing alkylperoxo complexes under neutral conditions in the absence of the alkyl hydroperoxide itself. As shown here, it specifically allows for the formation of alkylperoxo complexes that have hydrogen substituents on the α-carbon.

Details of how reactions 4 and 5 proceed deserve further comment and study. It is clear that the peroxo-bridged dimer, $PFe^{III}OOFe^{III}P$, which forms when PFe^{II} is treated with dioxygen,[38,39] is not created directly from the reaction of dioxygen with $PFe^{III}CHR_2$. This, along with the observations on the solution stability of $PFe^{III}CHR_2$ and the steric inhibition of the dioxygen insertion found for (TMP)$Fe^{III}CH_3$, argues against homolysis of the Fe–C bond preceding the dioxygen insertion.

For reaction 5, likely paths include homolysis of the O–O bond followed by rapid oxidation of the radical (path a, eq 7), a concerted path with O–O and C–H bond breaking occurring as the O–H bond is formed (path b, eq 7), or heterolysis of the O–O bond to give an oxidized ferryl complex at the peroxidase compound I level of oxidation and an alkoxide ion that rapidly loses hydride to the oxidized ferryl complex (path c, eq 7). Neither $PFe^{IV}{=}O$[40,41] nor $(P^{\bullet})Fe^{IV}{=}O$,[41,42] both of which have been detected by ^1H NMR studies on (TMP)Fe systems, is observed during these reactions. Likewise our attempt to stabilize the ferryl unit by interaction of a base (*N*-methylimidazole) with $PFe^{III}OOCHR_2$ has not led to the detection of (*N*-MeIm)-$PFe^{IV}{=}O$, which is stable and observable at −70 °C.[35,36] Hence, we conclude that the organic fragment is oxidized before it can escape from the proximity of the iron porphyrin environment.

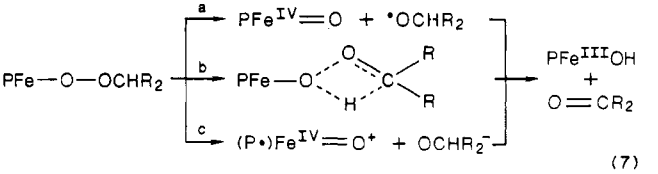

(7)

Our observations on dioxygen insertion allow for a second interpretation of the results of Corey and Walker on their biomimetic allylic oxidation.[18b] They report that sequential treatment of (3-phenylprop-2-enyl)tributyltin (**8**) with iron(III) bromide and dioxygen yields the ketone **11** via intermediates **9** and **10** (eq 8). However, the alternate possibility of conversion of **8** to **12** is entirely possible based on the observations made here, and the facility of direct insertion of dioxygen into Fe^{III}–C bonds should be noted.

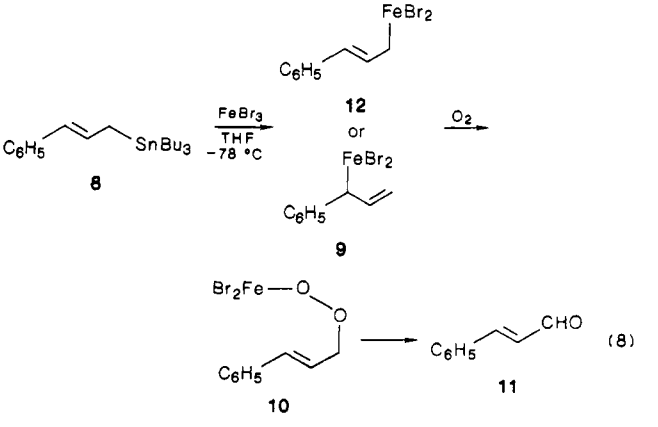

(8)

(37) Arasasingham, R. D.; Balch, A. L., unpublished results.

(38) Chin, D. H.; Del Gaudio, J. D.; La Mar, G. N.; Balch, A. L. *J. Am. Chem. Soc.* **1977**, *99*, 5486.

(39) Chin, D. H.; La Mar, G. N.; Balch, A. L. *J. Am. Chem. Soc.* **1980**, *102*, 4344.

(40) Balch, A. L.; Chan, Y.-W.; Cheng, R.-J.; La Mar, G. N.; Latos-Grazynski, L.; Renner, M. W. *J. Am. Chem. Soc.* **1984**, *106*, 7779.

(41) Balch, A. L.; Latos-Grazynski, L.; Renner, M. W. *J. Am. Chem. Soc.* **1985**, *107*, 2983.

(42) Groves, J. T.; Hanshalter, R. C.; Nakamura, M.; Nemo, T. E.; Evans, B. J. *J. Am. Chem. Soc.* **1981**, *103*, 2884.

The formation of acetaldehyde in the catalytic decomposition of ethyl hydroperoxide can be explained by the two steps given in eq 9 and 10. Figure 9 shows that it is possible to detect the

$$(TMP)Fe^{III}OH + C_2H_5OOH \rightarrow (TMP)Fe^{III}OOC_2H_5 + H_2O \quad (9)$$
(4′) (3′)

$$(TMP)Fe^{III}OOC_2H_5 \rightarrow (TMP)Fe^{III}OH + O{=}CHCH_3 \quad (10)$$
(3′) (4′)

alkylperoxo intermediate **3′** during this reaction, thus establishing an independent route (eq 9) for its formation. Equation 10, of course, is one of the three steps (eq 5) involved in the dioxygen/iron alkyl reaction. The formation of some ethanol in the catalytic decomposition probably results from a second pathway for the decomposition.

The catalysis of hydroperoxide dehydration is relevant to previous observations on the reactivity of hydroperoxides with a variety of heme proteins. Weller and Marnett noted that, in the presence of a reductant, 5-phenyl-4-pentenyl hydroperoxide was converted to 5-phenyl-4-pentenyl alcohol by several heme enzymes, including horseradish peroxidase, catalase, cytochrome *c* peroxidase, lactoperoxidase, and PGH synthase, in a normal peroxidase fashion.[20] However, with metmyoglobin, methemoglobin, and hematin alone, this hydroperoxide was decomposed catalytically to give a 5:1 ratio of 5-phenyl-4-pentenyl aldehyde to 5-phenyl-4-pentenyl alcohol without the need for a reductant.[20] At that point, the mechanism of aldehyde formation was not established, but now the two-step process (eq 9 and 10) readily accounts for these observations.

The differences between the behavior noted for the reactions of hydroperoxides with simple porphyrins (where dehydration occurs) and with the peroxidases (where O–O bond heterolytic cleavage occurs) underscore what has already been said many times regarding the active-site structure of the peroxidases. Hydrogen bonding to the coordinated peroxide and to the proximal imidazole (histidine) shown in A has been implicated in facilitating

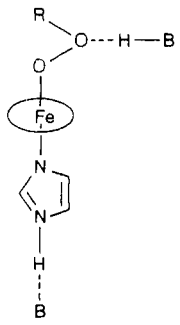

A

peroxide heterolysis to give ROH and $(P^{\bullet})Fe^{IV}{=}O^{+}$.[43] In studies such as the present one, where only a simple iron porphyrin is present, the complex network of hydrogen-bonding interactions is absent. Consequently, the course of the reaction is altered and with appropriate hydroperoxides, dehydration occurs.

Experimental Section

Materials. $TTPH_2$[47] and $TMPH_2$[48] were prepared by previously reported procedures and iron was inserted by the standard route. Toluene-d_8 (Aldrich) was deoxygenated by three freeze–pump–thaw cycles and stored over 4-Å sieves in a Vacuum Atmospheres glovebox under purified nitrogen. Methyl-, ethyl-, propyl-, isopropyl-, benzyl-, and (methyl-d_3)magnesium bromide and ethyl-d_5 iodide were purchased from Aldrich Chemical Co. Samples of $PFe^{III}CHR_2$ were prepared from the appropriate $PFe^{III}Cl$ and the Grignard reagent by an established procedure.[4] $(TTP)Fe^{III}CD_2CD_3$ was obtained by treating $(TTP)Fe$[14,27] with ethyl-d_5 iodide. All complexes were purified by chromatography (basic alumina with toluene as eluent) under subdued light in the Vacuum Atmospheres glovebox. Samples of $PFe^{III}OR$ and $(TMP)Fe^{III}OH$ were prepared by established methods.[26,31]

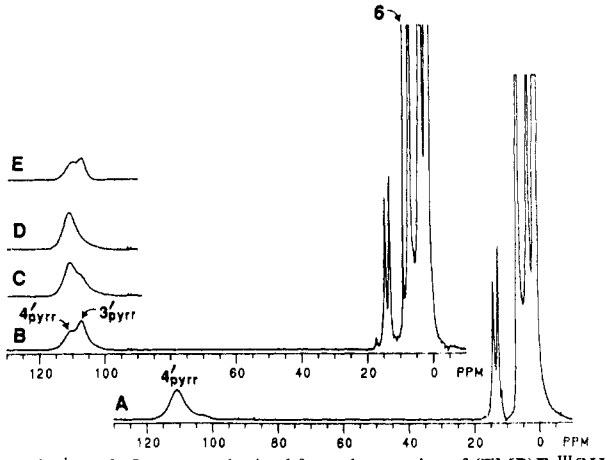

Figure 9. ^1H NMR spectra obtained from the reaction of $(TMP)Fe^{III}OH$ (5×10^{-3} M) (**4′**) with ethyl hydroperoxide at −60 °C in toluene-d_8 solution: (A) $(TMP)Fe^{III}OH$ before the addition of a tenfold excess of ethyl hydroperoxide; (B) the sample 10 min after the addition of ethyl hydroperoxide; (C) the same 30 min after the addition; (D) the same 70 min after the addition; (E) the same after the addition of a second portion of ethyl hydroperoxide. The peak labeled $3'_{pyrr}$ arises from $(TMP)Fe^{III}OOCH_2CH_3$ and that labeled 6 from acetaldehyde.

Reaction of $(TTP)Fe^{III}CHR_2$ (1) with Dioxygen. A toluene-d_8 solution of **1** was prepared under a nitrogen atmosphere, placed in an NMR tube capped with a rubber septum, and sealed with Parafilm. In a typical experiment, a 3 mM solution of **1** was cooled to −80 °C and dry dioxygen was introduced via a hypodermic needle. The sample was gently shaken and its color changed from red to dark green. The progress of the reaction was followed by NMR spectroscopy. The imidazole adducts were obtained by the addition (via syringe) of a solution of the ligand in toluene-d_8 to a toluene-d_8 solution of **1**.

Catalytic Decomposition of Ethyl Hydroperoxide. Ethyl hydroperoxide was synthesized by the reaction of ethyl methanesulfonate with hydrogen peroxide[49] and distilled under vacuum before use. ^1H NMR in toluene-d_8: 0.97 ppm, t, J = 7 Hz; 3.73 ppm, q. A toluene-d_8 solution of ethyl hydroperoxide (0.06 M) was added via syringe to an NMR tube containing a toluene-d_8 solution of (TMP)FeOH. The resulting (TMP)FeOH concentration was 10^{-4} M. The progress of the reaction was followed by NMR spectroscopy. After a 12-h period, three major species were observed: acetaldehyde (72%), ethanol (11%), and ethyl hydroperoxide (17%).

Instrumentation. NMR spectra were recorded on Nicolet NT-360 FT and NT-500 FT spectrometers operating in the quadrature mode (^1H frequencies are 360 and 500 MHz, respectively). The spectra were collected over a 40-kHz bandwidth with 16K data points and a 6-μs 90° pulse. For a typical paramagnetic spectrum, between 500 and 2000 transients were accumulated with a delay time of 50 ms, and for a typical diamagnetic spectrum, 16 transients were collected with a 2-s delay time. The signal-to-noise ratio was improved by apodization of the free induction decay. The residual methyl peak of toluene was used as a secondary reference, which was set at 2.09 ppm. To obtain line widths of overlapping resonances, the spectra were deconvoluted by using the NTC CAP routine of the Nicolet software.

Acknowledgment. We thank the National Institutes of Health (Grant GM 26226) for support. L.L.-G. was on leave from the University of Wrocław, Wrocław, Poland.

Registry No. 1-CH_3, 87607-82-7; **1**-C_2H_5, 110076-80-7; **1**-$CH(CH_3)_2$, 119907-37-8; **1**-CH_2Ph, 119907-38-9; **1**-OEt, 83970-56-3; **1**-n-C_3H_7, 119907-43-6; **2**, 19414-68-7; **3**-C_2H_5, 110076-82-9; **3′**-C_2H_5, 119907-44-7; **4**, 96503-21-8; **4′**, 77439-20-4; **5**, 11080-08-3; **7**, 119907-40-3; (TMP)$FeCH_3$, 110076-83-0; (*N*-MeIm)(TTP)$FeCH_3$, 119907-39-0; (TMP)$FeOCH_3$, 93842-72-9; (TMP)$FeOC(CH_3)_3$, 119907-41-4; (TMP)$FeOC_2H_5$, 119907-42-5; C_2H_5OOH, 3031-74-1; CH_3CHO, 75-07-0; C_2H_5OH, 64-17-5; O_2, 7782-44-7; CH_3CH_2CHO, 123-38-6; $(CH_3)_2C{=}O$, 67-64-1; PhCHO, 100-52-7; $(PhCH_2)_2$, 103-29-7; $H_2C{=}O$, 50-00-0.

(43) Peisach, J. *Ann. N.Y. Acad. Sci.* **1975**, *244*, 187.
(44) Poulos, T. L.; Kraut, J. *J. Biol. Chem.* **1980**, *255*, 8199.
(45) de Ropp, J. S.; Thanabal, V.; La Mar, G. N. *J. Am. Chem. Soc.* **1985**, *107*, 8268.
(46) Traylor, T. G.; Popovitz-Biro, R. *J. Am. Chem. Soc.* **1988**, *110*, 239.
(47) Adler, A. D.; Longo, F. R.; Kampus, F.; Kim, J. *J. Inorg. Nucl. Chem.* **1970**, *32*, 2443.
(48) Badger, G. M.; Jones, R. A.; Laslett, R. L. *Aust. J. Chem.* **1964**, *17*, 1028.
(49) Williams, H. R.; Mosher, H. S. *J. Am. Chem. Soc.* **1954**, *76*, 2984.